

Using precision coefficients on recurrence times and integrated currents to lower bound the average dissipation rate

Alberto Garilli* and Diego Frezzato

Department of Chemical Sciences, University of Padova, via Marzolo 1, I-35131, Padova, Italy.

(Dated: December 3, 2025)

For continuous-time Markov jump processes on irreducible networks and time-independent rate constants, we employ a transition-based formalism to express the long-time precision of a single integrated current over an observable channel in terms of precisions of the recurrence times of the forward and backward jumps, and of an effective affinity that captures the thermodynamic driving on that channel. This leads to a general lower bound for the stationary entropy production rate that extends the well-known Thermodynamic Uncertainty Relation (TUR). Such an augmented TUR, which incorporates the statistics of the recurrences, proves to be tighter than the standard one far from equilibrium, and potentially offers new opportunities for the optimization and design of biological and chemical out-of-equilibrium systems at the nanoscale.

I. INTRODUCTION

In small non-equilibrium systems, fluctuations play a crucial role and set fundamental constraints on performance. Stochastic thermodynamics provides the theoretical framework to quantify these limits, revealing how precision, speed, and energetic cost are tightly intertwined. A paradigmatic result in this direction is the Thermodynamic Uncertainty Relation (TUR) [1–4], which provides a quantitative link between fluctuations and dissipation.

For Markov jump processes on irreducible networks and reversible jumps, in particular, the TUR concerns a general lower bound to the precision of any time-integrated current. In this work, we shall focus on the integrated steady current $\mathcal{N}_t = \mathcal{N}_{\alpha \rightarrow \beta}^t - \mathcal{N}_{\beta \rightarrow \alpha}^t$, where $\mathcal{N}_{i \rightarrow j}^t$ indicates the total number of jumps $i \rightarrow j$ in a given time window of duration t , are bounded from below by dissipation. Denoting by

$$\mathcal{P}[X] = \frac{\langle X^2 \rangle - \langle X \rangle^2}{\langle X \rangle^2} \quad (1)$$

the squared coefficient of precision of a random variable X with non-zero mean, the bound reads

$$\mathcal{P}[\mathcal{N}_t] \geq \frac{2}{\sigma^{\text{ss}} t}, \quad (2)$$

revealing that higher precision (i. e. narrower fluctuations) of \mathcal{N}_t along any of the channels connecting the pair of states (α, β) requires higher dissipation, quantified by the (stationary) average entropy production rate σ^{ss} .

The TUR Eq. (2) represents a principle of broad relevance for biochemical networks and molecular machines [1, 2, 5–9]. Extensions of this idea also regard bounds on multiple output currents [10] and on other performance metrics. For example, lower bounds have been derived

for first-passage times [11] and their fluctuations [12] in Markov processes, for the number of coherent oscillations (and timing precision) in biochemical clocks [13, 14], and for information processing [15]. Similarly, the achievable signal-to-noise ratio of sensory readouts is fundamentally limited by dissipation [5]. In short, improving precision or speed in small systems inevitably incurs an irreducible thermodynamic cost.

Recent work has developed transition-based formulations of dissipation bounds when only partial information is available. In Ref. [16] it is demonstrated that the log-ratio of waiting-time distributions for forward and backward transitions encodes the cycle affinity, yielding a lower-bound estimator for the total entropy production. Similarly, any partial estimate of the entropy production rate, derived from the statistics of visible transitions, provides a value lower than σ^{ss} . These ideas have been extended into novel fluctuation relations. For instance, stopping an experiment after a fixed number of visible transitions recovers thermodynamic symmetry even in the presence of hidden dynamics [17], and coarse-grained fluctuation theorems have been formulated for multiple observable currents [18]. Universal trade-offs between entropy production and precision of counting observables or waiting times were also recently obtained [19].

In this context, we further elaborate on a recently introduced explicit formula for the precision coefficient of an extensive current at time t [20]. Employing a decomposition of the moments of the recurrence times in terms of the moments of inter-transition times between visible transitions, we obtain an exact expression of $\lim_{t \rightarrow \infty} t \mathcal{P}[\mathcal{N}_t]$ in terms of an effective affinity \mathcal{A} and of the precisions $\mathcal{P}[\tau_{\alpha \rightarrow \beta}]$, $\mathcal{P}[\tau_{\beta \rightarrow \alpha}]$ of the recurrence times of forward and backward transitions respectively. The affinity \mathcal{A} is the same that is obtained from the statistics of the sequences of observable transitions [17, 21]. Exploiting this fact, we provide a lower bound on the steady-state entropy production rate directly in terms of $\lim_{t \rightarrow \infty} t \mathcal{P}[\mathcal{N}_t]$, $\mathcal{P}[\tau_{\alpha \rightarrow \beta}]$ and $\mathcal{P}[\tau_{\beta \rightarrow \alpha}]$. This formulation links dissipation to experimentally accessible fluctuations of currents and recurrence times. The bound holds for any irreducible continuous-time Markov jump

* alberto.garilli@unipd.it

process and thus constrains the performance of nanoscale systems – for example, it sets a minimal entropy production required for a given precision in molecular motors or biochemical sensing networks [5].

II. FRAMEWORK

We consider a Markov jump process on an irreducible network with a finite number of states. We assume without loss of generality that pairs of states are connected by a single bidirectional transition channel with a time-independent transition rate constant k_{ij} from state i to state j and k_{ji} from j to i , ensuring that σ^{ss} is well defined at stationarity [22]. The state space probability \mathbf{p}_t evolves according to the master equation

$$\frac{d\mathbf{p}_t}{dt} = -\mathbf{R}\mathbf{p}_t, \quad (3)$$

with $[\mathbf{R}]_{ij} = -k_{ji}(1 - \delta_{ij}) + \delta_{ij} \sum_{n \neq i} k_{in}$ the rate matrix. For a pair of states α and β , we are interested in the extensive current

$$\mathcal{N}_t = \mathcal{N}_{\alpha \rightarrow \beta}^t - \mathcal{N}_{\beta \rightarrow \alpha}^t, \quad (4)$$

$\mathcal{N}_{i \rightarrow j}^t$ denoting the number of times the transition $i \rightarrow j$ occurs in a time window of duration t . Assuming that the system is initially found at stationarity, the integrated current \mathcal{N}_t is on average $\langle \mathcal{N}_t \rangle = Jt$ with J the stationary probability current $J = p_{\alpha}^{\text{ss}} k_{\alpha\beta} - p_{\beta}^{\text{ss}} k_{\beta\alpha} = F_{\alpha\beta} - F_{\beta\alpha}$, where $F_{ij} = p_i^{\text{ss}} k_{ij}$ is the stationary flux from i to j .

An exact formula for the precision coefficient $\mathcal{P}[\mathcal{N}_t]$ of an extensive current \mathcal{N}_t was recently found in Ref. [20]. In particular, denoting with $\epsilon = J/\omega$ the rectifying efficiency, with $\omega = F_{\alpha\beta} + F_{\beta\alpha}$ the dynamical activity (or traffic) along the observed channel, and introducing the coefficient $c_0 = (1 - \epsilon^2)/\epsilon^2$, for long observation times we have [20]

$$\begin{aligned} \mathcal{T}_{\infty} = \lim_{t \rightarrow \infty} t \mathcal{P}[\mathcal{N}_t] &= -\frac{1}{\epsilon J} + c_0 (\langle \tau_{\alpha \rightarrow \beta} | \alpha \rangle + \langle \tau_{\beta \rightarrow \alpha} | \beta \rangle) \\ &\quad + \frac{\mathcal{P}[\tau_{\alpha \rightarrow \beta}] - \mathcal{P}[\tau_{\beta \rightarrow \alpha}]}{J}. \end{aligned} \quad (5)$$

where the coefficients

$$\mathcal{P}[\tau_{i \rightarrow j}] = \frac{\langle \tau_{i \rightarrow j}^2 \rangle - \langle \tau_{i \rightarrow j} \rangle^2}{\langle \tau_{i \rightarrow j} \rangle^2}, \quad (6)$$

quantify the precision of the recurrence times $\tau_{i \rightarrow j}$, whose mean values satisfy $\langle \tau_{i \rightarrow j} \rangle = F_{ij}^{-1}$. The quantities $\langle \tau_{i \rightarrow j} | x_0 \rangle$ in Eq. (5), instead, represent the average occurrence times conditioned to the starting state x_0 .

The expression Eq. (5) represents our starting point: by employing the transition-based framework developed in Refs. [16–18, 21], we can derive a linear relation between the average recurrence times $\langle \tau_{i \rightarrow j} \rangle$ and the average conditional occurrence times $\langle \tau_{i \rightarrow j} | x_0 \rangle$. We briefly introduce the transition-based framework below.

III. VISIBLE TRANSITIONS' DYNAMICS

To simplify the notation, let $\ell \in \{\uparrow, \downarrow\}$ denote the visible transition in its two possible directions, $\uparrow: \alpha \rightarrow \beta$ and $\downarrow: \beta \rightarrow \alpha$, and let $\mathbf{s}(\ell)$ and $\mathbf{t}(\ell)$ denote the source and target states of ℓ respectively. The inverse transition $\bar{\ell}$ is obtained by swapping the source and target states of ℓ . Under the assumption that only the forward and backward jumps over the single monitored channel are observable, the time series of the output consists of sequences of transitions $\ell \in \{\uparrow, \downarrow\}$ and the inter-transition times $\tau_{\ell'\ell} := \tau_{\ell' \rightarrow \ell}$ [Fig. 1(c)].

It is a well established fact that sequences of single observable bidirectional transitions are generated by a discrete-time stochastic matrix \mathbf{P} whose elements are the trans-transition probabilities [17, 18, 21]

$$[\mathbf{P}]_{\ell\ell'} = p(\ell|\ell') = k(\ell)[\mathbf{S}^{-1}]_{\mathbf{s}(\ell)\mathbf{t}(\ell')}, \quad (7)$$

The trans-transition probability $p(\ell|\ell')$ is the probability that the next observed transition is $\ell \in \{\uparrow, \downarrow\}$ given that the previous one was $\ell' \in \{\uparrow, \downarrow\}$, regardless of the time between the two occurrences, with $k(\ell) = k_{\mathbf{s}(\ell)\mathbf{t}(\ell)}$ and $p(\ell|\ell') + p(\bar{\ell}|\ell') = 1$ [see Fig. 1(b)]. The matrix $\mathbf{S} := \mathbf{R}^{\setminus\{\uparrow, \downarrow\}}$ [23], also known as survival matrix, is obtained from the rate matrix \mathbf{R} as $[\mathbf{S}]_{ij} = [\mathbf{R}]_{ij}$ for all i, j except for $[\mathbf{S}]_{\alpha\beta} = [\mathbf{S}]_{\beta\alpha} = 0$. Given the trans-transition probabilities Eq. (7), we can define the effective affinity, or force,

$$\mathcal{A} = \log \frac{p(\uparrow|\uparrow)}{p(\downarrow|\downarrow)} \quad (8)$$

which drives the non-equilibrium current along the observed channel. The reduced effective entropy production rate

$$\sigma^{\ell} = J\mathcal{A}, \quad (9)$$

which is obtained solely from the observation of sequences of transitions regardless of the inter-transition times, lower bounds the stationary entropy production rate σ^{ss} of the full system, with equality holding for unicyclic networks [21].

Additionally, the knowledge of the probability density of the inter-transition times allows the estimation of an extra entropic contribution σ^{τ} related with transition-time asymmetries, providing the refined lower bound $\sigma^{\text{ss}} \geq \sigma^{\ell} + \sigma^{\tau}$ [21].

Interestingly, employing the transition based formalism we can provide a simple relation between the average recurrence times $\langle \tau_{i \rightarrow j} \rangle$ and the average occurrence times $\langle \tau_{i \rightarrow j} | i \rangle$ conditioned to the source state, appearing in Eq. (5), via the trans-transition probabilities Eq. (7). In the following section, we use this fact to derive our results.

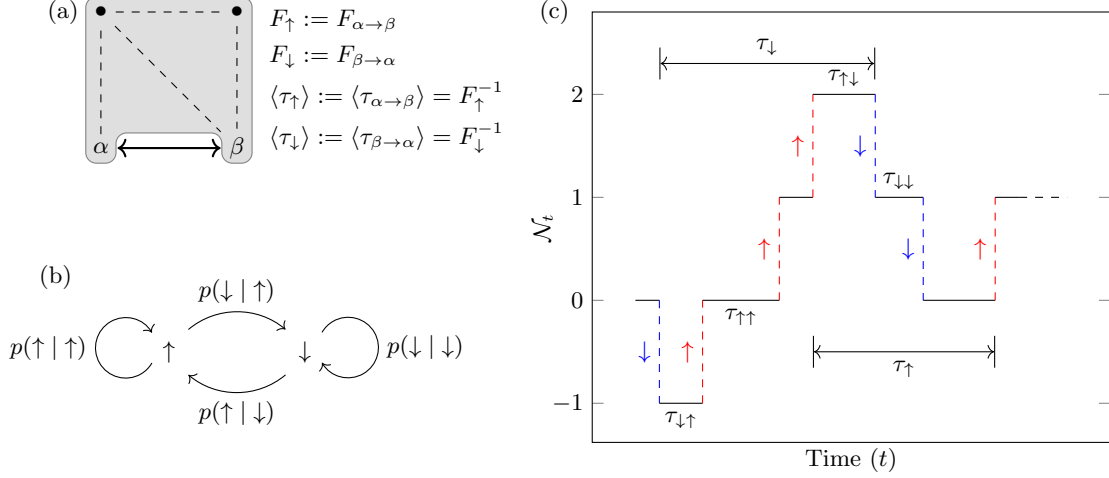


FIG. 1. (a) An example of Markov jump process where only bidirectional transitions along the channel connecting states α and β are observable. The shaded part thus represents the hidden part of the network. In this example, without loss of generality, only one channel $\alpha \rightarrow \beta$ is present; however, multiple channels connecting α and β may exist, and they can be incorporated in the hidden part of the network, or can be lumped together in a single observable channel. Additionally, we assume that each hidden channel is bidirectional, so that the entropy production rate σ^{ss} is well defined [22] and our results can be compared with the standard TUR Eq. (2). (b) Network of the effective process in the space of transitions. The sequence of transitions $\ell \in \{\uparrow, \downarrow\}$, with $\uparrow: \alpha \rightarrow \beta$ and $\downarrow: \beta \rightarrow \alpha$, is generated from the discrete-time process with transition matrix \mathbf{P} [see Eq. (7)]. (c) A typical realization of the process \mathcal{N}_t where only \uparrow and \downarrow are observed. Specifically, a transition \uparrow increases the integrated current \mathcal{N}_t by 1, whereas a transition \downarrow decreases the current by 1. Here, we also indicate the inter-transition times $\tau_{\ell'\ell}$ between successive occurrences of transitions ℓ' and ℓ , and the recurrence times τ_ℓ of transitions $\ell \in \{\uparrow, \downarrow\}$, which are blind to consecutive occurrences of the inverse transition $\bar{\ell}$.

IV. RESULTS

The moments of the inter-transition times are obtained in terms of the survival matrix \mathbf{S} [see Appendix A]. The recurrence times $\tau_{\alpha \rightarrow \beta}$ and conditional occurrence times $\tau_{\alpha \rightarrow \beta | x_0}$, on the other hand, are blind to the occurrences of the reverse transition $\beta \rightarrow \alpha$ between two occurrences of $\alpha \rightarrow \beta$ (the same holds for the inverse transition by swapping α and β). Therefore, they are expressed in terms of the survival matrix $\mathbf{S}' = \mathbf{R}^{\setminus \{\ell\}}$ with $[\mathbf{S}']_{ij} = [\mathbf{R}]_{ij}$ but with only $[\mathbf{S}']_{\alpha \rightarrow \beta} = 0$.

Let $\tau_{\ell | x_0}$ denote the occurrence time at which $\ell \in \{\uparrow, \downarrow\}$ occurs conditioned to an initial state x_0 . The recurrence time τ_ℓ is obtained from the conditional occurrence time by setting $x_0 = \mathbf{t}(\ell)$. We prove in Appendix A that

$$\langle \tau_{\ell | \mathbf{s}(\ell)} \rangle = \langle \tau_{\ell \ell} \rangle + \frac{p(\bar{\ell} | \bar{\ell})}{p(\ell | \bar{\ell})} \langle \tau_{\bar{\ell} \bar{\ell}} \rangle \quad (10)$$

with $\tau_{\ell' \ell}$ the time between transition ℓ' (first) and transition ℓ (next). The recurrence times thus satisfy

$$\langle \tau_\ell \rangle = p(\bar{\ell} | \ell) \left(\langle \tau_{\ell | \mathbf{s}(\ell)} \rangle + \langle \tau_{\bar{\ell} | \mathbf{s}(\bar{\ell})} \rangle \right), \quad (11)$$

which provides immediately that

$$\frac{\langle \tau_\ell \rangle}{\langle \tau_{\bar{\ell}} \rangle} = \frac{p(\bar{\ell} | \ell)}{p(\ell | \bar{\ell})} = \frac{F_{\bar{\ell}}}{F_\ell}, \quad (12)$$

where we used $\langle \tau_\ell \rangle = F_\ell^{-1}$, being F_ℓ the stationary flux along the direction of ℓ . As the ratio between forward

and backward fluxes is related with the local thermodynamic force \mathcal{F} , we straightforwardly obtain $\mathcal{F} = \log \frac{p(\uparrow | \downarrow)}{p(\downarrow | \uparrow)}$ choosing $\ell = \uparrow$ as the reference positive orientation of the transition.

To the best of our knowledge, Eqs. (10) to (12) are novel outcomes, the first one representing a direct proportionality between recurrence times and conditional occurrence times, the coefficient being expressed in terms of a trans-transition probability; the second one encodes the information of the local forces via the statistics of alternated series of visible transitions only.

In Appendix B we also provide explicit expressions for $\langle \tau_\ell^2 \rangle$ and $\langle \tau_{\ell | \mathbf{s}(\ell)}^2 \rangle$ in terms of trans-transition probabilities and first and second moments of the inter-transition times $\tau_{\ell' \ell}$.

Finally, let us consider the pair of states (α, β) and let $\uparrow := \alpha \rightarrow \beta$, $\downarrow := \beta \rightarrow \alpha$ along the considered channel connecting α and β . Also let $J = F_\uparrow - F_\downarrow$ denote the stationary current. From Eq. (11) we get

$$\langle \tau_{\uparrow | \alpha} \rangle + \langle \tau_{\downarrow | \beta} \rangle = \frac{\langle \tau_\uparrow \rangle - \langle \tau_\downarrow \rangle}{p(\downarrow | \uparrow) - p(\uparrow | \downarrow)} \quad (13)$$

$$= \frac{\langle \tau_\uparrow \rangle - \langle \tau_\downarrow \rangle}{p(\downarrow | \downarrow) - p(\uparrow | \uparrow)}, \quad (14)$$

where we used $p(\ell | \ell') = 1 - p(\bar{\ell} | \ell')$. The first and second terms in Eq. (5) can be grouped in a single term, yielding

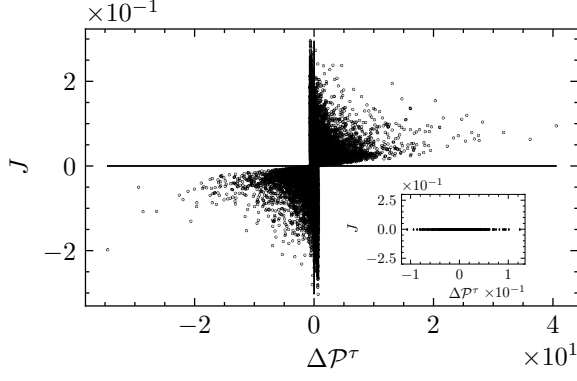


FIG. 2. Plot of J against $\Delta\mathcal{P}^\tau$ for 10^6 randomly generated instances of the network in Fig. 1(a). The rate constants were drawn as $k = 10^X$, where X is uniformly distributed in the interval $[-3, 0)$. Notably, there exist non-vanishing values of $\Delta\mathcal{P}^\tau$ for $J = 0$, which is associated to dissipation occurring in the hidden part of the network. As an example (in the inset), we generated several instances (10^3) of the same network where the α and β are now disconnected, with uniformly distributed rates between 0.1 and 1, so that $\mathbf{p}^{\text{stall}}$ is the stationary (stalling) probability of the process. $k_{\alpha\beta}$ and $k_{\beta\alpha}$ are then re-introduced from $k_{\alpha\beta} = k_{\beta\alpha} p_\beta^{\text{stall}} / p_\alpha^{\text{stall}}$ [28, 29], with $k_{\beta\alpha}$ uniformly distributed between 0.1 and 1, thereby ensuring that $J = 0$.

[see Appendix C]

$$\mathcal{T}_\infty = \frac{1}{J} \left(\frac{e^{\mathcal{A}} + 1}{e^{\mathcal{A}} - 1} + \mathcal{P}[\tau_\uparrow] - \mathcal{P}[\tau_\downarrow] \right), \quad (15)$$

where we used the definition Eq. (8) for the effective affinity \mathcal{A} . Recalling the effective entropy production rate $\sigma^\ell = J\mathcal{A} \leq \sigma^{\text{ss}}$ [21], we invert the expression above, obtaining our main result

$$\sigma^{\text{ss}} \geq 2J \coth^{-1}(J\mathcal{T}_\infty - \Delta\mathcal{P}^\tau), \quad (16)$$

with $\Delta\mathcal{P}^\tau = \mathcal{P}[\tau_\uparrow] - \mathcal{P}[\tau_\downarrow]$. Above, the quantity $J\mathcal{T}_\infty$ is also known as Fano factor [24–26]. Remarkably, the inequality (16) saturates for unicyclic networks because $\sigma^\ell = \sigma^{\text{ss}}$ in such a special case [16, 21]. Note that $\Delta\mathcal{P}^\tau$ can assume finite values even when $J = 0$, highlighting the presence of hidden dissipation [see the inset in Fig. 2]. Conversely J can be non-null even if $\Delta\mathcal{P}^\tau = 0$ [27]. Additionally, Eq. (16) yields the bound $|J\mathcal{T}_\infty - \Delta\mathcal{P}^\tau| > 1$ because $\coth^{-1}(x)$ is only defined for $|x| > 1$. This bound also follows directly from Eq. (5) by taking into account that $|\epsilon| < 1$.

The expression Eq. (16) reveals that a lower bound on the stationary entropy production rate σ^{ss} of the full system is obtained after evaluating the factor $\mathcal{T}_\infty = \lim_{t \rightarrow \infty} t \mathcal{P}[\mathcal{N}_t]$ at long times, and collecting the statistics of the recurrence times $\tau_{\alpha \rightarrow \beta}$ and $\tau_{\beta \rightarrow \alpha}$.

As a numerical check [see Fig. 3], we performed extensive tests on randomly generated networks to confirm that the bound Eq. (16) never falls above the true entropy production σ^{ss} . From the same plot, we see that

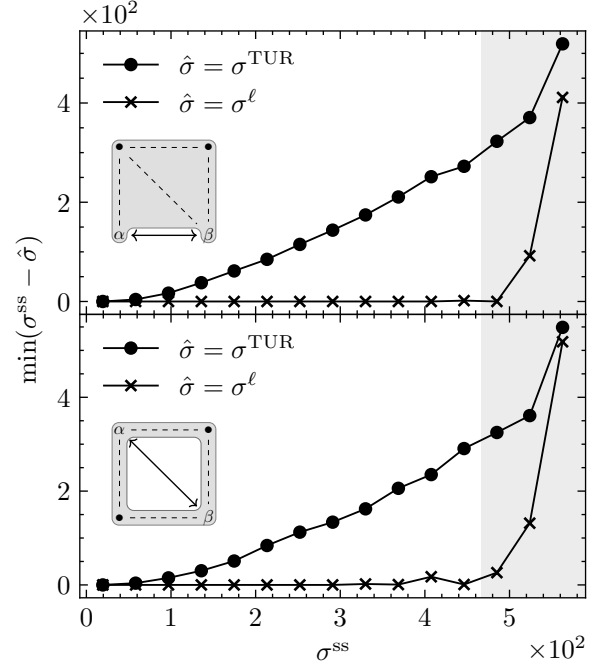


FIG. 3. Comparison between lower bounds for the entropy production rate σ^{ss} obtained from the long-time precision coefficient of a single integrated current: standard TUR [Eq. (2)] (circles) vs. asymptotic bound [Eq. (16)] (crosses). The points are obtained from the same instances as in Fig. 2. The values of σ^{ss} are divided into equally sized intervals. Then, for each interval, we pick the minimum value of the difference $\sigma^{\text{ss}} - \hat{\sigma}$, for $\hat{\sigma} = \sigma^{\text{TUR}}, \sigma^\ell$, with σ^ℓ corresponding to the right-hand side of Eq. (16). Each panel represents a different choice of observable edge for the same network, highlighted by the bidirectional arrow in the insets. This plot shows that while the TUR does not reach saturation as σ^{ss} grows, the bound Eq. (16) consistently saturates in a wide interval. The irregularities at very high σ^{ss} are due to statistical errors given by the limited amount of data falling in that region (less than 10 networks per interval, shaded region).

this bound outperforms the one obtained from the long-time TUR, especially far-from-equilibrium. In particular, the TUR estimate for σ^{ss} progressively worsens far from equilibrium, while the bound Eq. (16) can still approach saturation in the same regime.

V. DISCUSSION AND FINAL REMARKS

The bound $\sigma^\ell \leq \sigma^{\text{ss}}$ was originally formulated in terms of stalling probabilities [28–30] or from the statistics of sequences of visible transitions [17, 21], and it only accounts for asymmetries of extensive current-like quantities. Here we have rephrased this inequality in terms of directly measurable fluctuation statistics. Specifically, our main result, Eq. (16), involves the long-time precisions of a chosen integrated steady current \mathcal{N}_t and of the forward and backward recurrence times associated

with the corresponding transitions. This reformulation makes the connection between entropy production rate and measurable precision parameters explicit, thereby providing an augmented long-time TUR. It shows that one can infer a minimal steady-state entropy production rate from the asymptotic variability of the integrated current \mathcal{N}_t and the asymmetry in the recurrence-times fluctuations. The bound is meaningful whenever the reference current is nonzero, while for vanishing currents it reduces to the trivial inequality $\sigma^{\text{ss}} \geq 0$.

Unlike conventional TURs, which constrain current fluctuations alone, the present inequality yields a more stringent estimate of the dissipation rate. It remains effective even far from equilibrium, where the TUR becomes loose. In addition, Eq. (16) becomes exact for any unicyclic network with arbitrary rate constants, whereas the TUR saturates only under special conditions, as in the linear response regime or for unicyclic networks with homogeneous rates [1].

The structure of inequality Eq. (16) also opens a route for optimization. Since it couples the precision on the integrated current \mathcal{N}_t , recurrence-time precision, speed (i.e. the average current J), and dissipation rate, it provides a natural framework to study trade-offs among these quantities. For example, one may tune the rate constants to enhance the output's precision at the expense of higher energetic cost, or analyze the efficiency of molecular clocks and timers in terms of the balance between accuracy and dissipation. Such applications highlight how fluctuation-based bounds can go beyond inference and might serve as design principles for nonequilibrium processes.

The practical implications are broad. In biophysics, steady currents and recurrence-time distributions are often experimentally accessible, thanks to single-molecule tracking techniques, especially for rotary molecular motors (such as the F_1 -ATPase motor [31, 32]) and trans-

porters [8, 33, 34]. Furthermore, the randomness of catalytic sites in single-molecule enzymology is central in the field of statistical kinetics [24–26]. Because the bound Eq. (16) is expressed in terms of observable fluctuations, it provides a tangible route to quantify dissipation in complex systems where affinities or full state information remain hidden.

Looking forward, a particularly promising direction is to explore more deeply the information contained in forward and backward recurrence-time statistics. Asymmetries between these distributions encode irreversibility through their Kullback–Leibler divergence, potentially providing a direct microscopic link to entropy production. Here, we have shown that this information is already captured by differences in precision coefficients, suggesting a systematic way to detect dissipation even when average currents vanish. A detailed analysis of these temporal asymmetries beyond the second moments of the distributions might therefore sharpen the present bound and clarify the mechanisms by which hidden dynamics contribute to entropy production.

Overall, our contribution lies in rephrasing a known transition-based entropy production bound [Eq. (9)] in terms of measurable precision coefficients, thereby clarifying the role of both currents and recurrence-time fluctuations. This perspective not only strengthens thermodynamic inference but also highlights new opportunities for optimization and design, underscoring the relevance of precision-based bounds for the study of nonequilibrium processes in biological and chemical systems.

VI. ACKNOWLEDGEMENTS

The authors acknowledge the financial contribution from “Fondazione Cassa di Risparmio di Padova e Rovigo” (CARIPARO) within the framework of the project “NoneQ”, ID 68058.

-
- [1] A. C. Barato and U. Seifert, Thermodynamic uncertainty relation for biomolecular processes, *Phys. Rev. Lett.* **114**, 158101 (2015).
 - [2] T. R. Gingrich, J. M. Horowitz, N. Perunov, and J. L. England, Dissipation bounds all steady-state current fluctuations, *Physical Review Letters* **116**, 120601 (2016).
 - [3] P. Pietzonka, F. Ritort, and U. Seifert, Finite-time generalization of the thermodynamic uncertainty relation, *Physical Review E* **96**, 012101 (2017).
 - [4] J. M. Horowitz and T. R. Gingrich, Proof of the finite-time thermodynamic uncertainty relation for steady-state currents, *Physical Review E* **96**, 020103 (2017).
 - [5] K. Liu and J. Gu, Dynamical activity universally bounds precision of response in Markovian nonequilibrium systems, *Communications Physics* **8**, 62 (2025).
 - [6] Y. Song and C. Hyeon, Thermodynamic uncertainty relation to assess biological processes, *The Journal of Chemical Physics* **154** (2021).
 - [7] J. D. Mallory, O. A. Igoshin, and A. B. Kolomeisky, Do we understand the mechanisms used by biological systems to correct their errors?, *The Journal of Physical Chemistry B* **124**, 9289 (2020).
 - [8] P. Pietzonka, A. C. Barato, and U. Seifert, Universal bound on the efficiency of molecular motors, *Journal of Statistical Mechanics: Theory and Experiment* **2016**, 124004 (2016).
 - [9] W. Hwang and C. Hyeon, Energetic costs, precision, and transport efficiency of molecular motors, *The journal of physical chemistry letters* **9**, 513 (2018).
 - [10] A. Dechant, Multidimensional thermodynamic uncertainty relations, *Journal of Physics A: Mathematical and Theoretical* **52**, 035001 (2018).
 - [11] G. Falasco and M. Esposito, Dissipation-time uncertainty relation, *Physical Review Letters* **125**, 120604 (2020).

- [12] A. Pal, S. Reuveni, and S. Rahav, Thermodynamic uncertainty relation for first-passage times on Markov chains, *Phys. Rev. Res.* **3**, L032034 (2021).
- [13] L. Oberreiter, U. Seifert, and A. C. Barato, Universal minimal cost of coherent biochemical oscillations, *Physical Review E* **106**, 014106 (2022).
- [14] R. Marsland III, W. Cui, and J. M. Horowitz, The thermodynamic uncertainty relation in biochemical oscillations, *Journal of the Royal Society Interface* **16**, 20190098 (2019).
- [15] T. Kamijima, K. Funo, and T. Sagawa, Finite-time thermodynamic bounds and trade-off relations for information processing, *Physical Review Research* **7**, 013329 (2025).
- [16] J. Van der Meer, B. Ertel, and U. Seifert, Thermodynamic inference in partially accessible Markov networks: A unifying perspective from transition-based waiting time distributions, *Physical Review X* **12**, 031025 (2022).
- [17] P. E. Harunari, A. Garilli, and M. Polettini, Beat of a current, *Phys. Rev. E* **107**, L042105 (2023).
- [18] A. Garilli, P. E. Harunari, and M. Polettini, Fluctuation relations for a few observable currents at their own beat, *Journal of Physics A: Mathematical and Theoretical* **57**, 455003 (2024).
- [19] P. Pietzonka and F. Coghi, Thermodynamic cost for precision of general counting observables, *Phys. Rev. E* **109**, 064128 (2024).
- [20] A. Garilli and D. Frezzato, Interrelation between precisions on integrated currents and on recurrence times in Markov jump processes, *Physical Review E* **112**, 044141 (2025).
- [21] P. E. Harunari, A. Dutta, M. Polettini, and E. Roldán, What to learn from a few visible transitions' statistics?, *Phys. Rev. X* **12**, 041026 (2022).
- [22] J. Schnakenberg, Network theory of microscopic and macroscopic behavior of master equation systems, *Reviews of Modern physics* **48**, 571 (1976).
- [23] As explained in the main text, \mathbf{S} is obtained from the rate matrix \mathbf{R} by setting the matrix elements (α, β) and (β, α) to zero, without modifying its diagonal elements. Therefore, throughout the paper, we indicate with the symbol \setminus the removal of off-diagonal elements of a rate matrix associated to observable transitions. This should not be confused with stalling matrices [as in Refs. [28, 29]] where the corresponding rates are also canceled in the diagonal.
- [24] M. J. Schnitzer and S. Block, Statistical kinetics of processive enzymes, in *Cold Spring Harbor Symposia on Quantitative Biology*, Vol. 60 (Cold Spring Harbor Laboratory Press, 1995) pp. 793–802.
- [25] J. R. Moffitt and C. Bustamante, Extracting signal from noise: kinetic mechanisms from a Michaelis–Menten-like expression for enzymatic fluctuations, *The FEBS journal* **281**, 498 (2014).
- [26] J. R. Moffitt, Y. R. Chemla, and C. Bustamante, Methods in statistical kinetics, in *Methods in enzymology*, Vol. 475 (Elsevier, 2010) pp. 221–257.
- [27] For the very special case $\Delta\mathcal{P}^\tau = 0$, the bound Eq. (16) is tighter than the TUR, since $2J \coth^{-1}(J\mathcal{T}_\infty) > 2/\mathcal{T}_\infty$, when $|J\mathcal{T}_\infty| > 1$.
- [28] M. Polettini and M. Esposito, Effective thermodynamics for a marginal observer, *Physical review letters* **119**, 240601 (2017).
- [29] M. Polettini and M. Esposito, Effective fluctuation and response theory, *Journal of Statistical Physics* **176**, 94 (2019).
- [30] A. Raghu and I. Neri, Effective affinity for generic currents in Markov processes, *Journal of Statistical Physics* **192**, 50 (2025).
- [31] T. Watanabe-Nakayama, S. Toyabe, S. Kudo, S. Sugiyama, M. Yoshida, and E. Muneyuki, Effect of external torque on the ATP-driven rotation of F1-ATPase, *Biochemical and biophysical research communications* **366**, 951 (2008).
- [32] T. Mishima, D. Gupta, Y. Nakayama, W. C. Wareham, T. Ohyama, D. A. Sivak, and S. Toyabe, Efficiently driving F₁ molecular motor in experiment by suppressing nonequilibrium variation, *Physical Review Letters* **135**, 148402 (2025).
- [33] J. O. Wirth, L. Scheiderer, T. Engelhardt, J. Engelhardt, J. Matthias, and S. W. Hell, MINFLUX dissects the unimpeded walking of kinesin-1, *Science* **379**, 1004 (2023).
- [34] T. Deguchi, M. K. Iwanski, E.-M. Schentarra, C. Heidebrecht, L. Schmidt, J. Heck, T. Weihs, S. Schnorrenberg, P. Hoess, S. Liu, *et al.*, Direct observation of motor protein stepping in living cells using MINFLUX, *Science* **379**, 1010 (2023).
- [35] D. Frezzato, Stationary Markov jump processes in terms of average transition times: setup and some inequalities of kinetic and thermodynamic kind, *Journal of Physics A: Mathematical and Theoretical* **53**, 365003 (2020).

Appendix A: Proof of Eqs. (10) and (11)

Let $\uparrow: \alpha \rightarrow \beta$ be the transition from α to β through the chosen channel among the ones connecting α and β , and let $\downarrow: \beta \rightarrow \alpha$ be its reversed counterpart. Also let $\mathbf{S}' := \mathbf{R}^{\setminus\{\ell\}}$, $\ell \in \{\uparrow, \downarrow\}$, indicate the survival matrix derived for the first exit time problem where the given transition ℓ is absorbant, and let $\mathbf{S} := \mathbf{R}^{\setminus\{\uparrow, \downarrow\}}$ indicate the survival matrix where both \uparrow and \downarrow are absorbant.

According to our sign convention [see Eq. (3)], the average conditional occurrence time for transition ℓ is [20, 35]

$$\langle \tau_{\ell|x_0} \rangle = \sum_n \left[(\mathbf{S}')^{-1} \right]_{nx_0}. \quad (\text{A1})$$

Notice that the reverse transition $\bar{\ell}$ can occur arbitrarily many times before ℓ occurs.

Here we show that the average occurrence times can be expressed as a linear combination of the inter-transition times which are obtained from a first-exit problem where both \uparrow and \downarrow are absorbant, and therefore depend on the survival matrix \mathbf{S} . As stated in the main text, the four average inter-transition times $\langle \tau_{\ell'\ell} \rangle$ between consecutive transitions ℓ' and ℓ are [21]

$$\langle \tau_{\ell'\ell} \rangle = \frac{[\mathbf{S}^{-2}]_{\mathbf{s}(\ell)\mathbf{t}(\ell')}}{[\mathbf{S}^{-1}]_{\mathbf{s}(\ell)\mathbf{t}(\ell')}}, \quad (\text{A2})$$

where $\mathbf{s}(\ell)$ and $\mathbf{t}(\ell)$ represent the source and target states of transition ℓ .

Given an initial state x_0 at the initial time $t_0 = 0$, we are interested in the probability density $\rho(\tau, \ell|x_0)$ associated with the occurrence of ℓ in the time interval $[\tau, \tau + d\tau)$. Letting $\mathcal{N}(\bar{\ell})$ indicate the number of times $\bar{\ell}$ occurs before the occurrence of ℓ given x_0 , the density $\rho(\tau, \ell|x_0)$ can be decomposed as

$$\rho(\tau, \ell|x_0) = \sum_{n=0}^{\infty} \rho(\tau, \ell; \{\mathcal{N}(\bar{\ell}) = n\}|x_0) \quad (\text{A3})$$

where

$$\rho(\tau, \ell; \{\mathcal{N}(\bar{\ell}) = n\}|x_0) = \int_0^\tau dt_n \int_0^{t_n} dt_{n-1} \int_0^{t_{n-1}} dt_{n-2} \cdots \int_0^{t_2} dt_1 \rho(\tau, \ell; t_n, \bar{\ell}; t_{n-1}, \bar{\ell}; \cdots; t_1, \bar{\ell}|x_0) \quad (\text{A4})$$

is interpreted as a convolution of probability densities of the kind $[e^{-(t_i - t_{i-1})\mathbf{S}}]_{x, y_0} k_{xy}$, for suitable choices of the states x, y and y_0 [see below]. In what follows we treat separately the case where $x_0 = \mathbf{s}(\ell)$ and $x_0 = \mathbf{t}(\ell)$ and we study the problem by means of the Laplace transform $\mathcal{L}\{\rho\}$.

1. Case 1: $x_0 = \mathbf{s}(\ell)$

Let us consider the case $x_0 = \mathbf{s}(\ell)$. The integrand in Eq. (A4) becomes, for each n ,

$$\rho(\tau, \ell; t_n, \bar{\ell}; t_{n-1}, \bar{\ell}; \cdots; t_1, \bar{\ell}|\mathbf{s}(\ell)) = k(\ell) \left[e^{-(\tau - t_n)\mathbf{S}} \right]_{\mathbf{s}(\ell)\mathbf{s}(\ell)} (k(\bar{\ell}))^n \left(\prod_{i=1}^n \left[e^{-(t_i - t_{i-1})\mathbf{S}} \right]_{\mathbf{s}(\bar{\ell})\mathbf{s}(\ell)} \right), \quad (\text{A5})$$

with $t_0 = 0$. The Laplace transform of $e^{-t\mathbf{S}}$ reads

$$\int_0^\infty dt e^{-tu} e^{-t\mathbf{S}} = (u\mathbf{I} + \mathbf{S})^{-1} = \mathbf{S}(u)^{-1}, \quad (\text{A6})$$

with \mathbf{I} the identity matrix and where we defined $\mathbf{S}(u) = (u\mathbf{I} + \mathbf{S})$, which satisfies $\mathbf{S}(0) = \mathbf{S}$ and $\frac{d}{du} \mathbf{S}(-u)^{-1} = \mathbf{S}(-u)^{-2}$. The Laplace transform of Eq. (A3), by considering Eq. (A5) along with Eq. (A6), is then

$$\mathcal{L}\{\rho(\tau, \ell|\mathbf{s}(\ell))\}(u) = k(\ell) [\mathbf{S}(u)^{-1}]_{\mathbf{s}(\ell)\mathbf{s}(\ell)} \sum_{n=0}^{\infty} k(\bar{\ell})^n \left([\mathbf{S}(u)^{-1}]_{\mathbf{s}(\bar{\ell})\mathbf{s}(\ell)} \right)^n \quad (\text{A7})$$

By taking the derivative $(d\mathcal{L}(-u)/du)_{u=0}$ we obtain the average occurrence times Eq. (10) conditioned to the source state of ℓ :

$$\begin{aligned} \langle \tau_{\ell|\mathbf{s}(\ell)} \rangle &= \left(\frac{k(\ell) [\mathbf{S}(-u)^{-2}]_{\mathbf{s}(\ell)\mathbf{s}(\ell)}}{1 - k(\bar{\ell}) [\mathbf{S}(-u)^{-1}]_{\mathbf{s}(\bar{\ell})\mathbf{s}(\ell)}} \right)_{u=0} + \lim_{M \rightarrow \infty} \left(k(\ell) [\mathbf{S}(-u)^{-1}]_{\mathbf{s}(\ell)\mathbf{s}(\ell)} \frac{d}{du} \frac{1 - \left[k(\bar{\ell}) [\mathbf{S}(-u)^{-1}]_{\mathbf{s}(\bar{\ell})\mathbf{s}(\ell)} \right]^{M+1}}{1 - k(\bar{\ell}) [\mathbf{S}(-u)^{-1}]_{\mathbf{s}(\bar{\ell})\mathbf{s}(\ell)}} \right)_{u=0} \\ &= \frac{k(\ell) [\mathbf{S}^{-2}]_{\mathbf{s}(\ell)\mathbf{s}(\ell)}}{1 - k(\bar{\ell}) [\mathbf{S}^{-1}]_{\mathbf{s}(\bar{\ell})\mathbf{s}(\ell)}} + k(\ell) [\mathbf{S}^{-1}]_{\mathbf{s}(\ell)\mathbf{s}(\ell)} \left(\frac{k(\bar{\ell}) [\mathbf{S}^{-2}]_{\mathbf{s}(\bar{\ell})\mathbf{s}(\ell)}}{(1 - k(\bar{\ell}) [\mathbf{S}^{-1}]_{\mathbf{s}(\bar{\ell})\mathbf{s}(\ell)})^2} \right), \end{aligned} \quad (\text{A8}) \quad (\text{A9})$$

where we used the partial sum for the geometric series and then summed after taking $u = 0$. Finally, by considering that $\mathbf{s}(\ell) = \mathbf{t}(\bar{\ell})$ and by recognizing the inter-transition times Eq. (A2) and the trans-transition probabilities Eq. (7), we obtain Eq. (10):

$$\langle \tau_{\ell|\mathbf{s}(\ell)} \rangle = \langle \tau_{\bar{\ell}\ell} \rangle + \frac{p(\bar{\ell}|\bar{\ell})}{p(\ell|\bar{\ell})} \langle \tau_{\bar{\ell}\bar{\ell}} \rangle. \quad (\text{A10})$$

2. Case 2: $x_0 = \mathbf{t}(\ell)$

Similarly to the previous case, the Laplace transform of Eq. A3 for $x_0 = \mathbf{t}(\ell) = \mathbf{s}(\bar{\ell})$ reads

$$\mathcal{L}\{\rho(t, \ell | \mathbf{t}(\ell))\}(u) = k(\ell)[\mathbf{S}(u)^{-1}]_{\mathbf{s}(\ell)\mathbf{s}(\bar{\ell})} + k(\ell)k(\bar{\ell})[\mathbf{S}(u)^{-1}]_{\mathbf{s}(\ell)\mathbf{s}(\ell)}[\mathbf{S}(u)^{-1}]_{\mathbf{s}(\bar{\ell})\mathbf{s}(\bar{\ell})} \sum_{n=0}^{\infty} \left([\mathbf{S}(u)^{-1}]_{\mathbf{s}(\bar{\ell})\mathbf{s}(\ell)} \right)^n k(\bar{\ell})^n \quad (\text{A11})$$

Taking $(d\mathcal{L}(-u)/du)_{u=0}$ and using similar arguments to those used to get Eq. (A10) we obtain the average occurrence times conditioned to the target state of ℓ , which is exactly the average recurrence time $\langle \tau_\ell \rangle$ of transition ℓ . This corresponds to Eq. (11)

$$\langle \tau_\ell \rangle = p(\bar{\ell}|\ell) \left(\langle \tau_{\ell\bar{\ell}} \rangle + \langle \tau_{\bar{\ell}\ell} \rangle + \frac{p(\ell|\ell)}{p(\bar{\ell}|\ell)} \langle \tau_{\ell\ell} \rangle + \frac{p(\bar{\ell}|\bar{\ell})}{p(\ell|\bar{\ell})} \langle \tau_{\bar{\ell}\bar{\ell}} \rangle \right) \quad (\text{A12})$$

$$= p(\bar{\ell}|\ell) \left(\langle \tau_{\ell|\mathbf{s}(\ell)} \rangle + \langle \tau_{\bar{\ell}|\mathbf{s}(\bar{\ell})} \rangle \right). \quad (\text{A13})$$

Appendix B: Second moments of recurrence times and conditional occurrence times

Taking the second derivative $(d^2\mathcal{L}(-u)/du^2)_{u=0}$ of Eqs. (A7) and (A11), we obtain the second moments of the distributions of τ_ℓ and $\tau_{\ell|\mathbf{s}(\ell)}$ respectively. Using similar arguments to those used for Eqs. (A10) and (A13), we obtain

$$\langle \tau_\ell^2 \rangle = p(\bar{\ell}|\ell) \left(y + 2 \frac{p(\bar{\ell}|\bar{\ell})}{p(\ell|\bar{\ell})} \langle \tau_{\bar{\ell}\bar{\ell}} \rangle (\langle \tau_{\uparrow\downarrow} \rangle + \langle \tau_{\downarrow\uparrow} \rangle) + 2 \left(\frac{p(\bar{\ell}|\bar{\ell})}{p(\ell|\bar{\ell})} \right)^2 \langle \tau_{\bar{\ell}\bar{\ell}} \rangle^2 \right). \quad (\text{B1})$$

where

$$y = \langle \tau_{\downarrow\uparrow}^2 \rangle + \langle \tau_{\uparrow\downarrow}^2 \rangle + 2 \langle \tau_{\uparrow\downarrow} \rangle \langle \tau_{\downarrow\uparrow} \rangle + \frac{p(\uparrow|\uparrow)}{p(\downarrow|\uparrow)} \langle \tau_{\uparrow\uparrow}^2 \rangle + \frac{p(\downarrow|\downarrow)}{p(\uparrow|\downarrow)} \langle \tau_{\downarrow\downarrow}^2 \rangle, \quad (\text{B2})$$

which is independent of ℓ .

For the occurrence times conditioned to the source state of ℓ we find the second moments

$$\langle \tau_{\ell|\mathbf{s}(\ell)}^2 \rangle = \langle \tau_{\bar{\ell}\bar{\ell}}^2 \rangle + 2 \frac{p(\bar{\ell}|\bar{\ell})}{p(\ell|\bar{\ell})} \langle \tau_{\bar{\ell}\bar{\ell}} \rangle \langle \tau_{\bar{\ell}\ell} \rangle + \frac{p(\bar{\ell}|\bar{\ell})}{p(\ell|\bar{\ell})} \langle \tau_{\bar{\ell}\bar{\ell}}^2 \rangle + 2 \left(\frac{p(\bar{\ell}|\bar{\ell})}{p(\ell|\bar{\ell})} \right) \langle \tau_{\bar{\ell}\bar{\ell}} \rangle^2 \quad (\text{B3})$$

Appendix C: Proof of Eq. (15)

Given the stochastic matrix Eq. (7), the steady state of the transition space vector $\mathbf{q}^{\text{ss}} = (q_{\uparrow}^{\text{ss}}, q_{\downarrow}^{\text{ss}})^T$ is such that $\mathbf{q}^{\text{ss}} = \mathbf{P}\mathbf{q}^{\text{ss}}$. It can be easily verified that $q_{\uparrow}^{\text{ss}} = p(\uparrow|\downarrow)/(p(\uparrow|\downarrow) + p(\downarrow|\uparrow))$ and $q_{\downarrow}^{\text{ss}} = p(\downarrow|\uparrow)/(p(\uparrow|\downarrow) + p(\downarrow|\uparrow))$, from which we obtain the direct relation between the rectifying efficiency ϵ and \mathbf{q}^{ss} :

$$\epsilon = q^{\text{ss}}(\uparrow) - q^{\text{ss}}(\downarrow) = \frac{p(\uparrow|\downarrow) - p(\downarrow|\uparrow)}{p(\uparrow|\downarrow) + p(\downarrow|\uparrow)}. \quad (\text{C1})$$

Since the factor entering Eq. (5) can be expressed as

$$c_0 = \frac{2}{J} \frac{1}{\langle \tau_{\downarrow} \rangle - \langle \tau_{\uparrow} \rangle}, \quad (\text{C2})$$

by using Eq. (14) we obtain that

$$-\frac{1}{\epsilon J} + c_0(\langle \tau_{\uparrow|\alpha} \rangle + \langle \tau_{\downarrow|\beta} \rangle) = \frac{1}{J} \left(\frac{p(\uparrow|\uparrow) + p(\downarrow|\downarrow)}{p(\uparrow|\uparrow) - p(\downarrow|\downarrow)} \right) = \frac{1}{J} \left(\frac{e^{\mathcal{A}} + 1}{e^{\mathcal{A}} - 1} \right), \quad (\text{C3})$$

where we also used $p(\ell|\ell') = 1 - p(\bar{\ell}|\ell')$ and Eq. (8). Plugging the expression above into Eq. (5), we finally obtain Eq. (15).